Hmox1 (Heme Oxygenase-1) Protects Against Ischemia-Mediated Injury via Stabilization of HIF-1 (Hypoxia-Inducible Factor-1)

Dunn, Louise L.; Kong, Stephanie M. Y.; Tumanov, Sergey; Chen, Weiyu; Cantley, James; Ayer, Anita

Published in:
Arteriosclerosis, Thrombosis, and Vascular Biology

DOI:
10.1161/ATVBAHA.120.315393

Publication date:
2020

Document Version
Peer reviewed version

Heme oxygenase-1 protects against ischemia-mediated injury via stabilization of hypoxia-inducible factor-1α

Louise L. Dunn,[1,2,†] Stephanie M. Y. Kong[1,†], SergeyTumanov[1,3], Weiyu Chen,[1,2,3] James Cantley,[4] Anita Ayer,[1,2,3] Ghassan J Maghzal,[1,2] Robyn G. Midwinter,[5] Kim H. Chan,[3,6] Martin K. C. Ng,[3,6] Roland Stocker[1,2,3,5]

[1]The Victor Chang Cardiac Research Institute, Darlinghurst, NSW, Australia; [2]St Vincent's Clinical School, University of New South Wales, Sydney, Australia; [3]Heart Research Institute, Newtown, NSW, Australia; [4]University of Oxford, Oxford, England; [5]Centre for Vascular Research, School of Medical Sciences (Pathology), and Bosch Institute, Sydney Medical School, The University of Sydney, Sydney, Australia; [6]Royal Prince Alfred Hospital, Camperdown, NSW, Australia

[†]These authors contributed equally to this work

Running title: Heme Oxygenase-1 Modulates Response to Ischemia

Corresponding author: Professor Roland Stocker, Heart Research Institute, Newtown, NSW, 2042, Australia. Email: roland.stocker@hri.org.au; Phone: +61 2 8208 8900

Keywords: Metabolism, Cellular Reprogramming, Angiogenesis, Ischemia, Peripheral Vascular Disease

Subject codes: metabolism**,** cellular reprogramming**,** angiogenesis**,** ischemia**,** peripheral vascular disease

Total word count: 8,028 (Introduction, methods, results, conclusion, figure legends, references)

Total number of figures and tables: 6 figures, 2 supplemental tables, 4 supplemental figures

TOC category: basic

TOC subcategory: vascular biology

Abstract

Objective: Heme oxygenase-1 (Hmox1) is a stress-induced enzyme that catalyzes the degradation of heme to carbon monoxide, iron and biliverdin. Induction of Hmox1 and its products protect against cardiovascular disease, including ischemic injury. Hmox1 is also a downstream target of the transcription factor hypoxia-inducible factor-1α (HIF-1α), a key regulator of the body's response to hypoxia. However, the mechanisms by which Hmox1 confers protection against ischemia-mediated injury remain to be fully understood.

Approach and Results: Hmox1 deficient (*Hmox1*$^{-/-}$) mice had impaired blood flow recovery with severe tissue necrosis and auto-amputation following unilateral hind limb ischemia. Auto-amputation preceded the return of blood flow, and bone marrow transfer from littermate wild-type mice failed to prevent tissue injury and auto-amputation. In wild-type mice, ischemia-induced expression of Hmox1 in skeletal muscle occurred prior to stabilization of HIF-1α. Moreover, HIF-1α stabilization and glucose utilization were impaired in *Hmox1*$^{-/-}$ mice compared with wild-type mice. Experiments exposing dermal fibroblasts to hypoxia (1% O_2) recapitulated these key findings. Metabolomics analyses indicated a failure of *Hmox1*$^{-/-}$ mice to adapt cellular energy reprogramming in response to ischemia. Prolyl-4-hydroxylase inhibition stabilized HIF-1α in *Hmox1*$^{-/-}$ fibroblasts and ischemic skeletal muscle, decreased tissue necrosis and auto-amputation, and restored cellular metabolism to that of wild-type mice. Mechanistic studies showed that carbon monoxide stabilized HIF-1α in *Hmox1*$^{-/-}$ fibroblasts in response to hypoxia.

Conclusion: Our findings suggest that Hmox1 acts both downstream and upstream of HIF-1α, and that stabilization of HIF-1α contributes to Hmox1's protection against ischemic injury independent of neovascularization.

Non-standard abbreviations and acronyms:
DMOG, dimethyloxaloylglycine; Hmox1, heme oxygenase-1; PAD, peripheral arterial disease

Introduction

Critical limb ischemia and lower limb amputations represent the end stage of peripheral arterial disease (PAD) that affects >200 million patients worldwide.[1] Mortality rates for critical limb ischemia exceed those of other vascular occlusive diseases and mitigation of classic vascular risk factors has not substantially reduced the risk of amputation.[2] Moreover, randomized placebo-controlled trials of gene- and cell-based therapies that primarily target neovascularization have largely failed.[2] Given that the prevalence of PAD will continue to increase with the aging and growing diabetic populations new strategies aimed at prevention and management of critical limb ischemia are urgently required.

High plasma concentrations of bilirubin, a product of heme catabolism, are associated with protection against PAD and lower limb amputation. The National Health and Nutrition Examination Survey (NHANES) reported a 6% reduction in the odds of PAD for every ≈1.7 μmol/L increase in serum total bilirubin.[3] In the Fenofibrate and Event Lowering in Diabetes (FIELD) study, we reported an inverse association of baseline plasma bilirubin and the clinical endpoint of amputation in 9,795 type 2 diabetic patients.[4] Irrespective of placebo or fenofibrate treatment individuals with lower bilirubin had increased risk of amputation with a hazard ratio of 1.38 for every 5 μmol/L decrease in bilirubin. These studies build upon a body of literature implicating heme catabolism as being protective against cardiovascular diseases.[5]

Heme oxygenase-1 (Hmox1) catalyzes the degradation of heme to carbon monoxide, ferrous iron and biliverdin, which is then rapidly reduced to bilirubin by biliverdin reductase. Hmox1 is an inducible isoform of heme oxygenase whose transcription is triggered by a wide variety of stressors including heme, oxidative stress, UV irradiation and hypoxia. In pre-clinical models, induction of Hmox1 represents a crucial response of the cardiovascular system to injury and repair[5]. For example, pharmacological or gene therapy-mediated increase in Hmox1 inhibits vascular smooth muscle cell proliferation and intimal hyperplasia,[6, 7] promotes endothelial cell growth[8] and re-endothelialization,[9, 10] and provides long-term protection against ischemia/reperfusion injury in the heart.[11, 12] Similarly, Hmox1 gene transfer facilitates blood flow recovery and capillary density in hind limb ischemia,[13, 14] and administration of carbon monoxide[15, 16] and bilirubin[17] protect against hind limb ischemia-reperfusion injury. Conversely, Hmox1 deficiency or pharmacological inhibition of its enzymatic activity impairs angiogenesis and ischemia-mediated neovascularization in rodent models.[13, 14, 18, 19]

The adaptive response to ischemia entails a broad program of events that are driven, in part, via the transcription factor hypoxia inducible factor-1 (HIF-1). In response to low oxygen tensions the transcription factor targets genes involved in angiogenesis, glycolysis, and stress responses, including Hmox1.[20] However, it is becoming increasingly apparent that Hmox1 itself can exert effects on gene transcription[7, 21] and downstream energy metabolism[21], while carbon monoxide acts as a metabolic regulator in cancer cells.[22] While multiple lines of evidence support a protective role of Hmox1 against vascular ischemia, the mechanisms of protection it affords to the tissue served by the affected vascular bed remain unclear. As Hmox1 and HIF-1 are both increased in response to ischemia and associated with improved outcomes,[14, 18, 23-26] we thought it important to examine their interplay in an attempt to better understand how Hmox1 confers protection against ischemia-induced auto-amputation in a mouse hind limb model.

Materials and Methods

Experimental animals

All animal experiments were approved by the Garvan/St Vincent's Animal Ethics Committee and performed in accordance with the Australian Code for Care and Use of Animals for Scientific Purposes. *Hmox1*$^{+/-}$ breeding pairs on a BALB/c background were obtained from Dr Soares (Instituto de Gulbenkian de Ciencia, Portugal) from a colony originally generated by Dr Yet.[27] All mice used in these studies were bred at the Victor Chang Cardiac Research Institute BioCORE Facility (Darlinghurst, Australia) and the University of Sydney (Camperdown, Australia). Mice were housed in cage bedding (PrimeSafe, Australia) on a 12 h light/dark cycle with access to standard chow (rat and mouse premium breeder diet 23% protein, Gordons Specialty Feeds, NSW, Australia) and water *ad*

libitum.

Hind limb ischemia

Unilateral hind limb ischemia was surgically introduced in ~12-week-old male and female homozygous (*Hmox1*$^{-/-}$) mice, and sex-matched wild-type (*Hmox1*$^{+/+}$) and heterozygous (*Hmox1*$^{+/-}$) littermates, as described in Online Supplement. Where indicated, mice received dimethyloxaloylglycine (DMOG, 8 mg in 250 μL 0.9% saline) or vehicle by intra-peritoneal injection immediately prior to surgery then every second day.[28] Two observers blinded to genotype and treatment scored pedal reflexes and tissue injury as follows: 0, normal; 1, mild discoloration; 2, necrosis; 3, auto-amputation below the ankle; 4, auto-amputation above the ankle. The percentage of mice with auto-amputation was also determined at each time-point. Pedal reflexes in response to tail traction were scored as follows: 0, normal; 1, plantar flexion but not toe flexion; 2, no flexion; 3, dragging of the foot; 4, dragging of limb. Blood flow was measured non-invasively using a laser Doppler perfusion imager (moorLDI2-HIR, Moor Instruments, UK), as described in Online Supplement.

Bone marrow transplantation

Bone marrow was isolated from 6-12 weeks-old male *Hmox1*$^{+/+}$ or *Hmox1*$^{-/-}$ donor mice as described in Online Supplement. Male mice were used as donors so that their Y chromosome could be used to track engraftment and homing to sites of ischemia in female recipient mice. At 6 weeks of age, female *Hmox1*$^{+/+}$ or *Hmox1*$^{-/-}$ mice were irradiated (6.5 Gy) and 1×10^7 bone marrow donor cells administered in 200 μL by tail vein injection using a 25 G needle. After 6 weeks of bone marrow engraftment, female recipient mice underwent hind limb ischemia surgery. Donor bone marrow was male donor mice

Histological analyses

Gastrocnemii were removed, snap-frozen and cryosections (5 μm) obtained, as described in Online Supplement. Vessel density was assessed by anti-CD31-phycoerythrin, anti-smooth muscle actin-fluorescein isothiocyanate, and anti-laminin antibody, with Alexa Fluor 350. Photomicrographs were taken on the Zeiss Axio Imager M1 using the 20× objective (scale bar = 100 μm). Lumen diameter and CD31$^+$SMA$^+$ vessels and myocytes were enumerated by blinded observers. SMA$^+$-FITC vessels were classified by diameter (<50 μm, 50-100 μm, >100 μm).[29] A blinded veterinary pathologist (Rothwell Consulting, Sydney, Australia) assessed hind limb cell morphology. Apoptosis was assessed in serial sections of gastrocnemius by TUNEL (ApopTag® Peroxidase In Situ Apoptosis Detection Kit, Merck-Millipore, S7100) and anti-active caspase-3 antibody staining, as described in Online Supplement. Please see the Major Resources Table in the Supplemental Material for antibody details.

High-resolution respirometry

High-resolution respirometry was performed on red and white muscle fiber types, isolated from the medial head of the gastrocnemius, using the Oxygraph O2k system (Oroboros, Innsbruck, Austria) as described previously,[30] with measurements performed as described in Online Supplement. Oxygen concentration was kept above 250 μM with periodic addition of H_2O_2 (0.1 μM). The substrate-uncoupler-inhibition titration protocol was used to determine skeletal muscle respiration, and data were analyzed as described previously.[30]

Fibroblast isolation and treatment

Individual fibroblast lines were established from male *Hmox1*$^{+/+}$ (n=4) and *Hmox1*$^{-/-}$ (n=4) mice using a skin explant technique,[31] with the minor modifications described in Online Supplement. Fibroblasts were seeded at a density of 2×10^4/cm^2 and grown in standard tissue culture conditions. Culture media (DMEM + 20% FBS) was pre-equilibrated in a H35 Hypoxystation (Don Whitley Scientific, UK) at 1% O_2, 5% CO_2, nitrogen balance, 37 ºC with humidification. Fibroblasts were transferred to hypoxia conditions, media replaced with pre-equilibrated media and supplemented with 500 μM DMOG as indicated for the specified time period. For CORM-A1 studies, 5 μM CORM-A1 was re-suspended in water or inactivated (iCORM)[32]. Cells were lysed in sodium dodecyl sulfate

(SDS)-urea buffer for protein extraction.

Glucose uptake

For *ex vivo* assays, skeletal muscle glucose uptake was performed in soleus muscle as previously described[33] with amendments detailed in Online Supplement. Glucose uptake was calculated from the intracellular accumulation of [^{3}H]-2-deoxyglucose. For *in vitro* assays, fibroblasts were plated in a 12-well culture plate at 1×10^5 cells per well in 2 mL DMEM + 10% FBS. Cells were then transferred to the hypoxic chamber (1% O_2, 5% CO_2 at 37 °C humidified) or kept under standard tissue culture conditions. Glucose uptake was determined by liquid scintillation counting after 8 h incubation of cells with 2-[^{3}H]-deoxy-D-glucose as detailed in Online Supplement.

Biochemical assays

For plasma lactate, blood collected by cardiac puncture into lithium-heparin tubes was centrifuged at 2,000*g* for 15 min at 4 °C, and L-lactate assayed in plasma using a fluorimetric assay and following the manufacturer's protocol (Cayman Chemicals, 700510). Pyruvate and lactate were determined in cultured fibroblasts (1×10^6) by a fluorimetric assay following the manufacturer's protocol (Cayman Chemicals, 700470 (pyruvate), 700510 (lactate)). Biliverdin was determined in plantaris muscle by LC-MS/MS[34] as detailed in Online Supplement. ATP and AMP were determined by HPLC-UV[35] as detailed in Online Supplement. Metabolic and lipidomic analyses are described in the Online Supplement.

Protein isolation and Western blotting

Proteins were extracted in SDS-urea buffer and Western blots performed as described in Online Supplement using anti-HIF-1α, anti-Hmox1, anti-β-actin, or anti-α-tubulin antibody with anti-rabbit or anti-mouse horse radish peroxidase as secondary antibody. Lysates from mixed fiber-type gastrocnemius tissue were assessed using anti-HIF-1α with anti-mouse IRDye® 800 by LI-COR imaging (Odyssey Imager, Licor). X-ray film visualization was used to analyze lysates from cultured cells. Densitometry analyses were performed using Image Studio Lite version 5.2.5 (LI-COR Biosciences). Ponceau S staining was used for loading control and normalization of data[36]. Please see the Major Resources Table in the Supplemental Material for antibody details.

RNA isolation and qPCR

RNA was prepared using TRIzol reagent and qPCR performed using the SensiFast SYBR No-Rox kit (Bioline) and a LightCycler 480 (Roche), with primer sets detailed in Supplemental Table 1 and as described in Online Supplement. *Hmox1* was normalized to the average of three housekeeping genes (*Actb, 18s, Hrpt*) using the ΔΔCT method.[37]

Statistical analysis

Statistical analysis was performed using GraphPrism version 7 software. Results are expressed as mean ± standard error of the mean (SEM). Data was analyzed first for normality (D'Agostino-Pearson) and equal variance for continuous variables (excepting % survival curves). If passed, Student's t-test, Kruskal-Wallis one-way ANOVA or two-way ANOVA were performed with pos hoc tests for between group comparisons where appropriate. For two group comparisons where either test failed the Mann-Whitney rank sum test was used. $P<0.05$ was considered as statistically significant.

Results

Hmox1 deficiency is associated with ischemia-induced auto-amputation

To determine the role of Hmox1 in hind limb ischemia, we utilized *Hmox1*$^{+/+}$ and *Hmox1*$^{-/-}$ littermate mice on a BALB/c background, where the oxygen concentration in ischemic tissue more closely resembles the value in critical limb ischemia patients with imminent amputation.[38, 39] Compared with C57BL/6, BALB/c mice also possess a lower capacity for compensatory collateral artery growth after femoral artery occlusion.[39-41] Following induction of unilateral hind limb ischemia, *Hmox1*$^{-/-}$ mice had increased tissue necrosis and auto-amputation as early as 3 days after ischemia, and impairment of pedal reflexes compared with *Hmox1*$^{+/+}$ mice (Figures 1A-D, Online Figure IA).

There were no significant differences in auto-amputation, tissue injury or pedal reflexes between *Hmox1*$^{+/+}$ mice and *Hmox1*$^{+/-}$ littermates (Online Figure IB-D). Hematoxylin and eosin staining of gastrocnemius tissue 24 h after ischemia displayed features consistent with necrosis (*e.g.*, eosinophilic swollen myocytes with loss of nuclei) while apoptosis assessed by TUNEL and active caspase-3 staining was negligible (Online Figure IE). These data indicate that the *Hmox1* allele confers protection against ischemia-induced necrosis and auto-amputation.

Non-invasive laser Doppler perfusion monitoring (Figure 1E) demonstrated that blood flow recovery was significantly impaired in *Hmox1*$^{-/-}$ compared with wild-type littermate mice at 17 and 21 days after ischemia (Figure 1F), *i.e.*, 2 weeks after the onset of auto-amputation. Hmox1 deficiency also significantly decreased the density of blood vessels with diameters of 50-100 μm and >100 μm in gastrocnemius tissue 21 days after ischemia (Figure 1G), while smaller arterioles were not affected. These results confirm a previous study reporting Hmox1 deficiency to attenuate blood flow recovery after hind limb ischemia in C57BL/6 mice.[14] What is novel, however, is that hind limb ischemia caused auto-amputation in *Hmox1*$^{-/-}$ mice on BALB/c but not C57BL/6 genetic background, and that auto-amputation preceded impaired blood flow recovery, suggesting that *Hmox1* deficiency in non-vascular tissue of BALB/c mice contributed to ischemia-induced auto-amputation.

Bone marrow Hmox1 does not rescue auto-amputation

To directly assess the contribution of vascular Hmox1 to the auto-amputation phenotype, bone marrow transfer experiments were performed. Lethally irradiated female *Hmox1*$^{-/-}$ and *Hmox1*$^{+/+}$ mice were reconstituted with male *Hmox1*$^{+/+}$ bone marrow cells and, after a period of 6 weeks, unilateral hind limb ischemia was introduced. Twenty-one days after hind limb ischemia, bone marrow engraftment and migration of progenitors to the site of ischemia was confirmed by PCR detection of the *sex determining region-Y* gene in ischemic plantaris of female recipients (Online Figure IIA). Transfer of wild-type bone marrow to *Hmox1*$^{-/-}$ mice modestly (from 78 to 57%) decreased but did not prevent auto-amputation compared with non-irradiated *Hmox1*$^{-/-}$ mice (compare Figure 2A with Figure 1B). Also, wild-type bone marrow transfer failed to significantly improve tissue injury, pedal reflexes, neovascularization, and blood perfusion (Figure 2B-E, Online Figure IIB). These results indicate that bone marrow Hmox1 and by inference, bone marrow-facilitated neovascularization, was not a primary factor responsible for prevention of ischemia-induced tissue necrosis and auto-amputation in *Hmox1*$^{+/+}$ mice, consistent with ischemia-induced auto-amputation preceding blood flow recovery in *Hmox1*$^{-/-}$ mice.

Ischemia-mediated changes in energy metabolism is altered in *Hmox1* deficient mice

We next compared metabolic activity in skeletal muscle of *Hmox1*$^{+/+}$ and *Hmox1*$^{-/-}$ mice without (naïve) and with hind limb ischemia. We first determined mitochondrial respiration in red and white fibers of the gastrocnemius by high-resolution respirometry.[30, 42] In red fibers of naïve *Hmox1*$^{+/+}$ and *Hmox1*$^{-/-}$ mice, maximal oxygen flux as well as electron transfer capacity through complex I, complex II, and electron transferring flavoprotein, or when oxidative phosphorylation was uncoupled were comparable (Figure 3A, B). By comparison, oxygen consumption was negligible in white fibers of naïve mice of both genotypes (Online Figure IIIA), consistent with these fibers exhibiting a glycolytic phenotype. We next determined *ex vivo* [^{3}H]-2-deoxyglucose uptake in soleus from naïve mice. Naïve *Hmox1*$^{-/-}$ mice had significantly elevated [^{3}H]-2-deoxyglucose uptake compared with *Hmox1*$^{+/+}$ littermates (Figure 3C), indicating that Hmox1 deficiency increases glucose demand.

Three days after ischemia, *i.e.*, the time point at which auto-amputation occurred first, respiration was essentially undetectable in the ischemic muscle of *Hmox1*$^{+/+}$ and *Hmox1*$^{-/-}$ mice (Figure 3D, E). [^{3}H]-2-deoxyglucose uptake was increased in both genotypes, although *Hmox1*$^{-/-}$ mice had a significantly decreased capacity to increase glucose uptake relative to that observed in naïve mice (Figure 3F, G). Moreover, plasma lactate was significantly lower in *Hmox1*$^{-/-}$ compared with *Hmox1*$^{+/+}$ mice (Figure 3H). Time-course studies revealed a rapid loss in mitochondrial respiration in red gastrocnemius fibers of *Hmox1*$^{+/+}$ mice as early as 30 min after ischemia, with negligible respiration remaining by 3 h (Online Figure IIIC). This was associated with an increase in the tissue AMP-to-ATP ratio (Online Figure IIID), indicative of the deteriorating oxidative energy metabolism.

In light of this rapid loss of mitochondrial respiration in ischemic tissue, we also examined red fibers from the gastrocnemius of the sham-operated, non-ischemic right hind limb 3 days after resection of the femoral artery: mitochondrial respiration was repressed in *Hmox1*$^{-/-}$ compared with *Hmox1*$^{+/+}$ mice (Figure 3I). This suggested that hind limb ischemia induced a systemic stress and that Hmox1 was required to maintain normal mitochondrial respiration under these conditions. In support of this notion, Hmox1 expression was induced in the sham-operated right hind limb of ischemic *Hmox1*$^{+/+}$ compared with naïve *Hmox1*$^{+/+}$ mice (Figure 3J). Together, these data indicate that *Hmox1* deficiency perturbs skeletal glucose uptake and utilization as well as mitochondrial respiration in response to ischemia, suggesting that Hmox1 may play a role in ischemia-mediated metabolic reprogramming.

Ischemia-mediated HIF-1α expression is blunted in *Hmox1* deficient mice

In light of the metabolic perturbations observed in *Hmox1*$^{-/-}$ mice in response to ischemia, we next examined the expression of HIF-1α, as this subunit regulates the heterodimeric transcription factor HIF-1 that itself mediates adaptive responses to tissue hypoxia.[43] We used a mixed population of fibers across the proximal portion of the gastrocnemius, since the expression of HIF-1α[44] and Hmox1[45] varies across different skeletal muscle fiber types. As expected, HIF-1α protein expression was significantly increased in ischemic skeletal muscle from *Hmox1*$^{+/+}$ mice 3 days after ischemia (Figure 4A). Strikingly, this response was blunted in *Hmox1*$^{-/-}$ mice (Figure 4A). At the same time, Hmox1 protein was increased in ischemic skeletal muscle of *Hmox1*$^{+/+}$ but not *Hmox1*$^{-/-}$ mice (Figure 4B), consistent with the presence of a hypoxia response element in the promoter of the Hmox1 gene and Hmox1 being a known down-stream target of HIF-1.[20] Increased Hmox1 protein expression was associated with increased endogenous Hmox activity, as assessed by the increase in skeletal muscle content of biliverdin, determined by LC-MS/MS (Figure 4C).

Time-course studies revealed that substantive expression of HIF-1α in ischemic gastrocnemius was not observed during the first 16 h of ischemia, *i.e.*, the time period within which oxidative energy metabolism becomes blunted, in sharp contrast to the strong induction seen after 72 h ischemia (Figure 4A). In contrast to HIF-1α, *Hmox1* mRNA and protein increased significantly as early as 3 and 6 h after ischemia, respectively in *Hmox1*$^{+/+}$ mice (Figure 4B, D). As expected, *Hmox1* mRNA and protein were not detected in skeletal muscle of *Hmox1*$^{-/-}$ mice before or after ischemia (Figure 4D). These data indicate that during the initial 16 h of ischemia, expression of Hmox1 protein precedes and is independent of HIF-1α stabilization.

Hypoxia-induced HIF-1α stabilization and energy metabolism are impaired in *Hmox1* deficient fibroblasts

To further explore the relationship between Hmox1, HIF-1α stabilization and energy metabolism under low oxygen tensions, we utilized dermal fibroblasts isolated from the dorsum of *Hmox1*$^{-/-}$ and *Hmox1*$^{+/+}$ littermate mice. In wild-type fibroblasts, Hmox1 protein expression increased time-dependently in response to hypoxia (1% O_2), while Hmox1 was not detected in fibroblasts from *Hmox1*$^{-/-}$ mice (Figure 5A). Consistent with the hind limb ischemia data (Figure 4A), *Hmox1*$^{+/+}$ fibroblasts had significantly increased HIF-1α stabilization in response to hypoxia compared with cells from *Hmox1*$^{-/-}$ mice (Figure 5B). Importantly, hypoxia-mediated induction of Hmox1 protein also preceded significant HIF-1α stabilization in wild-type fibroblasts (1 h for Hmox1, Figure 5A; 3 h for HIF-1α, Figure 5B). Furthermore, wild-type fibroblasts responded to hypoxia by significantly increased uptake of [^{3}H]-2-deoxyglucose (Figure 5C), with associated increases in cellular pyruvate and lactate (Figure 5D and E), whereas *Hmox1* deficient fibroblasts failed to increase glucose uptake, pyruvate and lactate in response to hypoxia. Collectively, these data suggest that Hmox1 induction is upstream of, and in part required, for HIF-1α stabilization and metabolic reprogramming in response to hypoxia.

Stabilization of HIF-1α rescues ischemia-induced auto-amputation in *Hmox1*$^{-/-}$ mice

We next sought to determine if the observed decrease in HIF-1α stabilization in ischemic skeletal muscle could account for the hypoxia-induced auto-amputation in *Hmox1*$^{-/-}$ mice, making use of dimethyloxaloylglycine (DMOG). DMOG is an analog of 2-oxoglutarate that stabilizes HIF-1α by

competitively inhibiting prolyl and asparaginyl hydroxylases, and that has been used successfully in a variety of animal models.[28, 46] DMOG significantly increased HIF-1α in fibroblasts from *Hmox1*$^{-/-}$ mice exposed to normoxia (0 h time point) and hypoxia (Figure 6A). Similar to DMOG, exposure of fibroblasts from *Hmox1*$^{-/-}$ mice to the carbon monoxide-releasing molecule A1 (CORM-A1) but not inactivated CORM-A1 (iCORM) significantly increased HIF-1α in response to hypoxia (Figure 6B).

Similar to the situation with isolated fibroblasts, administration of DMOG to *Hmox1*$^{-/-}$ mice resulted in a significant increase in HIF-1α protein in ischemic muscle 3 weeks after ischemia (Figure 6C). We administered DMOG immediately prior to inducing ischemia, then every other day until tissue collection to avoid feedback loops in the HIF-1 pathway.[28] Importantly, DMOG significantly decreased auto-amputation (Figure 6D) and tissue injury (Figure 6E) in *Hmox1*$^{-/-}$ mice subjected to hind limb ischemia, whereas DMOG had no material effect on blood flow recovery (Figure 6F). Preliminary metabolomic and lipidomic analyses of hind limb gastrocnemius muscle of *Hmox1*$^{+/+}$ and *Hmox1*$^{-/-}$ mice ± DMOG treatment 5 days after ischemia indicated that Hmox1 deficiency significantly increased 1-carbon metabolism and tricarboxylic acid cycle intermediates while tissue concentrations of nicotinamide and triglycerides were decreased (Figure 6G, Online Figure IVA, Online Supplemental Table II). DMOG treatment reversed these metabolic abnormalities (Figure 6H, Online Figure IVB).

Discussion

Our study identifies a role for Hmox1 in HIF-1α stabilization in response to hypoxia. We show that mice deficient in *Hmox1* have impaired HIF-1α stabilization and metabolic abnormalities in ischemic skeletal muscle, and that this is associated with auto-amputation of the afflicted limb. Pharmacological stabilization of HIF-1α rescues ischemia-induced auto-amputations and tissue necrosis, and it normalizes metabolic disturbances in *Hmox1*$^{-/-}$ mice. In wild-type skeletal muscle and isolated fibroblasts, ischemia and hypoxia induce Hmox1 protein prior to HIF-1α stabilization. While Hmox1 has been known as a downstream target of HIF-1α, our data suggest a new paradigm for the interplay between Hmox1 and this transcription factor, in which Hmox1 contributes to the regulation of the response to hypoxia by also acting upstream of HIF-1α.

Hmox1 is induced rapidly in response to a wide variety of stressors and it plays a key role in cellular protection.[5] The key finding of the current study, *i.e.*, that induction of Hmox1 expression preceded HIF-1α stabilization in response to low oxygen tensions and that Hmox1 can work upstream of a transcription factor in addition to being its downstream target, is not without precedent. We have shown previously that chemically distinct Hmox1 inducers and plasmid-mediated Hmox1 over-expression increase the Janus-like transcription factor Ying Yang-1 (YY1) in vascular smooth muscle cells, and that YY1 itself induces Hmox1.[7] Similar to the HIF-1α stabilization reported here, carbon monoxide (CO) increased YY1 expression.[7] Others reported CO to induce Hmox1 by increasing nuclear translocation of the transcription factor Nrf2,[47] while hypoxia-mediated nuclear-localization of Hmox1 has been shown to activate both Nrf2[21] and AP1[48]. Thus, our current observations add further weight to an emerging body of evidence that implicates Hmox1 in coordinating transcriptional responses.

The mechanism by which Hmox1 increases HIF-1α to protect against ischemic injury is the subject of future investigations. Increased Hmox1 expression in the ischemic tissue was associated with increased heme degradation to biliverdin (Figure 4C) while exogenously added CO, another product of heme oxygenase activity, promoted HIF-1α stabilization in fibroblast exposed to hypoxia (Figure 6B). These findings suggest that Hmox1 enzymatic activity is required for HIF-1α stabilization, although our studies did not test whether the observed increase in HIF-1α stabilization was direct or indirect. Otterbein and colleagues reported CO gas (250 ppm) to induce the expression of HIF-1α in murine macrophages *in vitro* and mouse lungs *in vivo* under normoxic conditions.[49] In that study, CO was unable to induce HIF-1α expression in mitochondria-deficient macrophages, and hydrogen peroxide (H_2O_2) alone increased HIF-1α expression while the inclusion of the H_2O_2-

metabolizing enzyme catalase attenuated the ability of CO to increase HIF-1α.[49] The implied role of mitochondria-derived H_2O_2 in promoting HIF-1α expression by CO is supported by the observation that mitochondrial H_2O_2 increases as a result of CO binding to cytochrome aa_3,[50] although this non-canonical mechanism of HIF-1α stabilization remains controversial[51] just as the molecular details of how mitochondrial H_2O_2 increases HIF-1α remain obscure. As an alternative mechanism, CO could inhibit HIF-1α ubiquitination by enhancing its interaction with the chaperone, heat shock protein-90.[52] Irrespective of the underlying mechanism, it is known is that administration of exogenous CO protects rat[16] and mouse[15] hind limb muscle from ischemia-reperfusion injury, and the data presented here suggest that this may extend to endogenous CO, produced by Hmox1 in the ischemic muscle.

HIF-1 initiates a broad set of transcription programs coordinating neovascularization, glycolysis and stress responses. Consistent with this, DMOG was reported to increase vessel density in the hind limb of C57BL/6 mice, and this was associated with HIF-1α stabilization.[28] Also, combined gene therapies of Hmox1 and HIF-1α improved neovascularization and limb salvage following ischemia in wild-type C57BL/6 mice over single therapy.[26] Similarly, combined *Hmox1* and *Vegfa* gene therapy decreased the incidence of necrotic toes in wild-type[14] and *Hmox1*$^{-/-}$[53] C57BL/6 mice, while pharmacological inhibition of Hmox1 impaired blood flow recovery and increased limb necrosis in C57BL/6 mice[18] and mice heterozygous for the *HIF-1α* null allele have decreased blood flow recovery and limb salvage following ischemia.[23] By comparison, using mice exclusively on a BALB/c strain background we observed modest improvements in ischemia-mediated neovascularization and blood flow recovery in *Hmox1*$^{-/-}$ animals whether they were reconstituted with wild-type bone marrow or treated with DMOG. The BALB/c strain background is well known to have increased tissue necrosis, and diminished *Vegfa* expression and collateral networks in response to ischemia[40, 54] when compared to the C57BL/6 strain. Indeed, we did not detect significant induction of *Vegfa* in either *Hmox1*$^{+/+}$ or *Hmox1*$^{-/-}$ mice in response to ischemia (not shown). Our observations suggest that increasing Hmox1 can protect against ischemic injury via the HIF-1α pathway independent of substantial improvement of neovascularization.

Given the divergence between neovascularization and tissue necrosis in the present investigation, we examined the role of Hmox1 in HIF-1α mediated glucose utilization. Notably, we found that impaired HIF-1α stabilization in *Hmox1*$^{-/-}$ mice was associated with diminished capacity of the skeletal muscle to increase glucose uptake and its utilization in response to ischemia. These observations were echoed in isolated fibroblasts. We further observed ischemic injury to elicit a remote response in the contralateral limb of *Hmox1*$^{-/-}$ by modulating cellular energy metabolism.

Current management and treatment approaches for PAD have not led to a substantial reduction in the risk of amputation over the past 30 years.[18] Moreover, larger randomized placebo-controlled trials of angiogenic gene-orientated and cell-based therapies have failed to translate promising pre-clinical targets.[2] This suggests that promoting neovascularization alone is insufficient to prevent the sequelae and consequence of limb ischemia, specifically amputation. In the present study, we observed skeletal muscle biliverdin IXα concentrations to significantly increase in *Hmox1*$^{+/+}$ but not *Hmox1*$^{-/-}$ mice after three days of ischemia, a time point that coincided with the onset of auto-amputations. As the biliverdin IXα detected in *Hmox1*$^{-/-}$ mice could only come from constitutively active Hmox2, our findings also imply that Hmox2 alone is not sufficient to prevent auto-amputations. It is important to note that tissue biliverdin is the direct product of Hmox activity while plasma bilirubin is only a surrogate. Nevertheless, our mouse study recapitulates the key observation reported in the FIELD study, namely an inverse association between plasma bilirubin concentrations and lower limb amputation.[4] What remains to be determined is whether bilirubin, a potent antioxidant itself conveys the protection against auto-amputations observed in this study. At the least, it is a potential biomarker for risk of non-traumatic lower limb amputations in type 2 diabetes.

While our data indicate a novel relationship between Hmox1 and HIF-1α in protecting against ischemia-induced auto-amputations, species- and tissue-specific effects should be considered. In mouse and rat cells it has been shown consistently that hypoxia induces HIF-1α, which can activate

the hypoxia response element within the *Hmox1* promoter. Conversely, in human cells the response is varied, with hypoxia increasing *HMOX1* expression in dermal fibroblasts but failing to do so in multiple endothelial cell types.[56] These observations may be explained, in part, by the presence or relative absence of Bach1, a hypoxia-induced repressor of *HMOX1* transcription.[57] In the current study we utilized DMOG as a proof-of-principle tool to enhance HIF-1α stability in skeletal muscle and prevent auto-amputations in *Hmox1*$^{-/-}$ mice. DMOG normalized several metabolic abnormalities observed in the ischemic skeletal muscle of *Hmox1*$^{-/-}$ mice. Of the latter, the decrease in serine and methionine in Hmox1 deficiency provides separate evidence for Hmox1 being upstream of HIF-1α, as HIF-1α activates the serine/1-carbon metabolism pathway.[58] Also, HIF-1α inhibits the TCA cycle[59] and fatty acid β-oxidation,[60] so that a comparatively more active TCA cycle and β-oxidation in *Hmox1*$^{-/-}$ than WT mice could explain the observed increase and decrease in TCA intermediates and triglycerides, respectively. As hypoxia decreases NAD^+,[61] the finding that Hmox1 deficiency further decreases nicotinamide is consistent with *Hmox1*$^{-/-}$ mice already experiencing an element of hypoxic stress. While we did not examine the effect of DMOG on HIF-1α stability in the endothelium, neurons and circulating inflammatory cells, previous studies confirmed the broad specificity of DMOG[46, 62, 63] Thus, our current study does not specifically delineate the role of skeletal muscle HIF-1α in protecting against auto-amputation in the absence of Hmox1.

In summary, we report a novel role for skeletal muscle Hmox1 in which it stabilizes HIF-1α and promotes effective glucose utilization to limit ischemia-induced tissue necrosis and auto-amputations. Moreover, pharmacological stabilization of HIF-1α in *Hmox1* deficiency limits ischemia-induced tissue necrosis and prevents auto-amputations. Insights obtained from our current study may have important implications for critical limb ischemia, cardiovascular disease in general, and other pathologies in which oxygen supply and energy metabolism are perturbed.

Acknowledgements
The authors would like to acknowledge the technical assistance of Darren Newington, Alice Rothwell, Cacang Suarna, Kelsey Fisher-Wellman, Jacqueline Stöckli and David James.

Sources of Funding
The research was funded by the National Health and Medical Research Council of Australia Program Grant 1052616 to RS, Project Grant 1050776 to RS and MKCN, Senior Principal Research Fellowship 1111632 to RS, and Early Career Fellowship 537537 to LLD. KHC received a scholarship from the National Heart Foundation (PC 08S 4127) and the Royal Australian College of Physicians. The authors also thank New South Wales Government Office for Health and Medical Research.

Disclosures
None.

References

1. Fowkes FGR, Rudan D, Rudan I, Aboyans V, Denenberg JO, McDermott MM, Norman PE, Sampson UKA, Williams LJ, Mensah GA and Criqui MH. Comparison of global estimates of prevalence and risk factors for peripheral artery disease in 2000 and 2010: a systematic review and analysis. *Lancet*. 2013;382:1329-1340.
2. Teraa M, Conte MS, Moll FL and Verhaar MC. Critical limb ischemia: current trends and future directions. *J Am Heart Assoc*. 2016;5:e002938.
3. Perlstein TS, Pande RL, Beckman JA and Creager MA. Serum total bilirubin level and prevalent lower-extremity peripheral arterial disease: National Health and Nutrition Examination Survey (NHANES) 1999 to 2004. *Arterioscler Thromb Vasc Biol*. 2008;28:166-172.
4. Chan KH, O'Connell RL, Sullivan DR, Hoffmann LS, Rajamani K, Whiting M, Donoghoe MW, Vanhala M, Hamer A, Yu B, Stocker R, Ng MK and Keech AC. Plasma total bilirubin levels predict amputation events in type 2 diabetes mellitus: the Fenofibrate Intervention and Event Lowering in Diabetes (FIELD) study. *Diabetologia*. 2013;56:724-736.
5. Ayer A, Zarjou A, Agarwal A and Stocker R. Heme oxygenases in cardiovascular health and disease. *Physiol Rev*. 2016;96:1449-1508.
6. Duckers HJ, Boehm M, True AL, Yet S-F, San H, Park JL, Webb RC, Lee M-E, Nable GJ and Nabel EG. Heme oxygenase-1 protects against vascular constriction and proliferation. *Nat Med*. 2001;7:693-698.
7. Beck K, Wu BJ, Ni J, Santiago FS, Malabanan KP, Li C, Wang Y, Khachigian LM and Stocker R. Interplay between heme oxygenase-1 and the multifunctional transcription factor yin yang 1 in the inhibition of intimal hyperplasia. *Circ Res*. 2010;107:1490-1497.
8. Abraham NG, Scapagnini G and Kappas A. Human heme oxygenase: cell cycle-dependent expression and DNA microarray identification of multiple gene responses after transduction of endothelial cells. *J Cell Biochem*. 2003;90:1098-1111.
9. Lau AK, Leichtweis SB, Hume P, Mashima R, Hou JY, Chaufour X, Wilkinson B, Hunt NH, Celermajer DS and Stocker R. Probucol promotes functional reendothelialization in balloon-injured rabbit aortas. *Circulation*. 2003;107:2031-2036.
10. Tanous D, Bräsen JH, Choy K, Wu BJ, Kathir K, Lau A, Celermajer DS and Stocker R. Probucol inhibits in-stent thrombosis and neointimal hyperplasia by promoting re-endothelialization. *Atherosclerosis*. 2006;189:342-349.
11. Wang G, Hamid T, Keith RJ, Zhou G, Partridge CR, Xiang X, Kingery JR, Lewis RK, Li Q, Rokosh DG, Ford R, Spinale FG, Riggs DW, Srivastava S, Bhatnagar A, Bolli R and Prabhu SD. Cardioprotective and antiapoptotic effects of heme oxygenase-1 in the failing heart. *Circulation*. 2010;121:1912-1925.
12. Li Q, Guo Y, Ou Q, Wu WJ, Chen N, Zhu X, Tan W, Yuan F, Dawn B, Luo L, Hunt GN and Bolli R. Gene transfer as a strategy to achieve permanent cardioprotection II: rAAV-mediated gene therapy with heme oxygenase-1 limits infarct size 1 year later without adverse functional consequences. *Basic Res Cardiol*. 2011;106:1367-1377.
13. Suzuki M, Iso-o N, Takeshita S, Tsukamoto K, Mori I, Sato T, Ohno M, Nagai R and Ishizaka N. Facilitated angiogenesis induced by heme oxygenase-1 gene transfer in a rat model of hindlimb ischemia. *Biochem Biophys Res Commun*. 2003;302:138-143.
14. Jazwa A, Stepniewski J, Zamykal M, Jagodzinska J, Meloni M, Emanueli C, Jozkowicz A and Dulak J. Pre-emptive hypoxia-regulated HO-1 gene therapy improves post-ischaemic limb perfusion and tissue regeneration in mice. *Cardiovascular research*. 2013;97:115-124.
15. Patel R, Albadawi H, Steudel W, Hashmi FF, Kang J, Yoo HJ and Watkins MT. Inhalation of carbon monoxide reduces skeletal muscle injury after hind limb ischemia-reperfusion injury in mice. *Am J Surg*. 2012;203:488-95.
16. Bihari A, Cepinskas G, Forbes TL, Potter RF and Lawendy AR. Systemic application of carbon monoxide-releasing molecule 3 protects skeletal muscle from ischemia-reperfusion injury. *J Vasc Surg*. 2017;66:1864-1871.

17. Adin CA, Croker BP and Agarwal A. Protective effects of exogenous bilirubin on ischemia-reperfusion injury in the isolated, perfused rat kidney. *Am J Physiol Renal Physiol*. 2005;288:F778-F784.
18. Tongers J, Knapp JM, Korf M, Kempf T, Limbourg A, Limbourg FP, Li Z, Fraccarollo D, Bauersachs J, Han X, Drexler H, Fiedler B and Wollert KC. Haeme oxygenase promotes progenitor cell mobilization, neovascularization, and functional recovery after critical hindlimb ischaemia in mice. *Cardiovascular research*. 2008;78:294-300.
19. Grochot-Przeczek A, Kotlinowski J, Kozakowska M, Starowicz K, Jagodzinska J, Stachurska A, Volger OL, Bukowska-Strakova K, Florczyk U, Tertil M, Jazwa A, Szade K, Stepniewski J, Loboda A, Horrevoets AJG, Dulak J and Jozkowicz A. Heme oxygenase-1 is required for angiogenic function of bone marrow-derived progenitor cells: role in therapeutic revascularization. *Antioxid Redox Signal*. 2014;20:1677-1692.
20. Lee PJ, Jiang BH, Chin BY, Iyer NV, Alam J, Semenza GL and Choi AM. Hypoxia-inducible factor-1 mediates transcriptional activation of the heme oxygenase-1 gene in response to hypoxia. *J Biol Chem*. 1997; 272:5375-5381.
21. Biswas C, Shah N, Muthu M, La P, Fernando AP, Sengupta S, Yang G and Dennery PA. Nuclear heme oxygenase-1 (HO-1) modulates subcellular distribution and activation of Nrf2, impacting metabolic and anti-oxidant defenses. *J Biol Chem*. 2014;289:26882-26894.
22. Yamamoto T, Takano N, Ishiwata K, Ohmura M, Nagahata Y, Matsuura T, Kamata A, Sakamoto K, Nakanishi T, Kubo A, Hishiki T and Suematsu M. Reduced methylation of PFKFB3 in cancer cells shunts glucose towards the pentose phosphate pathway. *Nat Commun*. 2014;5:3480.
23. Bosch-Marce M, Okuyama H, Wesley JB, Sarkar K, Kimura H, Liu YV, Zhang H, Strazza M, Rey S, Savino L, Zhou YF, McDonald KR, Na Y, Vandiver S, Rabi A, Shaked Y, Kerbel R, Lavallee T and Semenza GL. Effects of aging and hypoxia-inducible factor-1 activity on angiogenic cell mobilization and recovery of perfusion after limb ischemia. *Circ Res*. 2007;101:1310-8.
24. Lin HH, Chen YH, Chang PF, Lee YT, Yet SF and Chau LY. Heme oxygenase-1 promotes neovascularization in ischemic heart by coinduction of VEGF and SDF-1. *J Mol Cell Cardiol*. 2008;45:44-55.
25. Czibik G, Sagave J, Martinov V, Ishaq B, Sohl M, Sefland I, Carlsen H, Farnebo F, Blomhoff R and Valen G. Cardioprotection by hypoxia-inducible factor 1 alpha transfection in skeletal muscle is dependent on haem oxygenase activity in mice. *Cardiovascular research*. 2009;82:107-14.
26. Bhang SH, Kim JH, Yang HS, La WG, Lee TJ, Kim GH, Kim HA, Lee M and Kim BS. Combined gene therapy with hypoxia-inducible factor-1α and heme oxygenase-1 for therapeutic angiogenesis. *Tissue Eng Part A*. 2011;17:915-26.
27. Yet SF, Layne MD, Liu X, Chen YH, Ith B, Sibinga NE and Perrella MA. Absence of heme oxygenase-1 exacerbates atherosclerotic lesion formation and vascular remodeling. *The Journal of physiology*. 2003;17:1759-1761.
28. Milkiewicz M, Pugh CW and Egginton S. Inhibition of endogenous HIF inactivation induces angiogenesis in ischaemic skeletal muscles of mice. *J Physiol*. 2004;560:21-26.
29. Simons M, Alitalo K, Annex BH, Augustin HG, Beam C, Berk BC, Byzova T, Carmeliet P, Chilian W, Cooke JP, Davis GE, Eichmann A, Iruela-Arispe ML, Keshet E, Sinusas AJ, Ruhrberg C, Woo YJ and Dimmeler S. State-of-the-art methods for evaluation of angiogenesis and tissue vascularization: a scientific statement from the American Heart Association. *Circ Res*. 2015;116:e99-e132.
30. Pesta D and Gnaiger E. High-resolution respirometry: OXPHOS protocols for human cells and permeabilized fibers from small biopsies of human muscle. *Methods Mol Biol*. 2012;810:25-58.
31. Harford JB. Preparation and isolation of cells. *Curr Protoc Cell Biol*. 2006;32:2.0.1-2.0.2.
32. Motterlini R, Sawle P, Hammad J, Bains S, Alberto R, Foresti R and Green CJ. CORM-A1: a new pharmacologically active carbon monoxide-releasing molecule. *The Journal of physiology*. 2005;19:284-286.

33. Li J, Cantley J, Burchfield JG, Meoli CC, Stöckli J, Whitworth PT, Pant H, Chaudhuri R, Groffen AJ, Verhage M and James DE. DOC2 isoforms play dual roles in insulin secretion and insulin-stimulated glucose uptake. *Diabetologia*. 2014;57:2173-2182.
34. Chen W, Maghzal GJ, Ayer A, Suarna C, Dunn LL and Stocker R. Absence of the biliverdin reductase-a gene is associated with increased endogenous oxidative stress. *Free Radic Biol Med*. 2018;115:156-165.
35. Huang H, Yan Y, Zuo Z, Yang L, Li B, Song Y and Liao L. Determination of adenosine phosphates in rat gastrocnemius at various postmortem intervals using high performance liquid chromatography. *J Forensic Sci*. 2010;55:1362-1366.
36. Fortes MA, Marzuca-Nassr GN, Vitzel KF, da Justa Pinheiro CH, Newsholme P and Curi R. Housekeeping proteins: How useful are they in skeletal muscle diabetes studies and muscle hypertrophy models? *Anal Biochem*. 2016;504:38-40.
37. Pfaffl MW. A new mathematical model for relative quantification in real-time RT-PCR. *Nucleic Acids Res*. 2001;29:e45.
38. Ubbink DT, Spincemaille GH, Reneman RS and Jacobs MJ. Prediction of imminent amputation in patients with non-reconstructible leg ischemia by means of microcirculatory investigations. *J Vasc Surg*. 1999;30:114-121.
39. Helisch A, Wagner S, Khan N, Drinane M, Wolfram S, Heil M, Ziegelhoeffer T, Brandt U, Pearlman JD, Swartz HM and Schaper W. Impact of mouse strain differences in innate hindlimb collateral vasculature. *Arterioscler Thromb Vasc Biol*. 2006;26:520-526.
40. Chalothorn D, Clayton JA, Zhang H, Pomp D and Faber JE. Collateral density, remodeling, and VEGF-A expression differ widely between mouse strains. *Physiol Genomics*. 2007;30:179-191.
41. Schmidt CA, Ryan TE, Lin CT, Inigo MMR, Green TD, Brault JJ, Spangenburg EE and McClung JM. Diminished force production and mitochondrial respiratory deficits are strain-dependent myopathies of subacute limb ischemia. *J Vasc Surg*. 2017;65:1504-1514.
42. Jacobs RA, Diaz V, Meinild AK, Gassmann M and Lundby C. The C57Bl/6 mouse serves as a suitable model of human skeletal muscle mitochondrial function. *Exp Physiol*. 2013;98:908-921.
43. Semenza GL. Targeting HIF-1 for cancer therapy. *Nat Rev Cancer*. 2003;3:721-732.
44. Pisani DF and Dechesne CA. Skeletal muscle HIF-1α expression is dependent on muscle fiber type. *J Gen Physiol*. 2005;126:173-178.
45. Vesely MJ, Exon DJ, Clark JE, Foresti R, Green CJ and Motterlini R. Heme oxygenase-1 induction in skeletal muscle cells: hemin and sodium nitroprusside are regulators in vitro. *Am J Physiol*. 1998;275:C1087-C1094.
46. Ockaili R, Natarajan R, Salloum F, Fisher BJ, Jones D, Fowler AA, 3rd and Kukreja RC. HIF-1 activation attenuates postischemic myocardial injury: role for heme oxygenase-1 in modulating microvascular chemokine generation. *Am J Physiol Heart Circ Physiol*. 2005;289:H542-H548.
47. Wang B, Cao W, Biswal S and Dore S. Carbon monoxide-activated Nrf2 pathway leads to protection against permanent focal cerebral ischemia. *Stroke*. 2011;42:2605-2610.
48. Lin Q, Weis S, Yang G, Weng YH, Helston R, Rish K, Smith A, Bordner J, Polte T, Gaunitz F and Dennery PA. Heme oxygenase-1 protein localizes to the nucleus and activates transcription factors important in oxidative stress. *J Biol Chem*. 2007;282:20621-20633.
49. Chin BY, Jiang G, Wegiel B, Wang HJ, Macdonald T, Zhang XC, Gallo D, Cszimadia E, Bach FH, Lee PJ and Otterbein LE. Hypoxia-inducible factor 1α stabilization by carbon monoxide results in cytoprotective preconditioning. *Proc Natl Acad Sci USA*. 2007;104:5109-5114.
50. Piantadosi CA. Carbon monoxide, reactive oxygen signaling, and oxidative stress. *Free Radic Biol Med*. 2008;45:562-569.
51. Movafagh S, Crook S and Vo K. Regulation of hypoxia-inducible factor-1α by reactive oxygen species: new developments in an old debate. *J Cell Biochem*. 2015;116:696-703.
52. Choi YK, Kim CK, Lee H, Jeoung D, Ha KS, Kwon YG, Kim KW and Kim YM. Carbon monoxide promotes VEGF expression by increasing HIF-1α protein level via two distinct

mechanisms, translational activation and stabilization of HIF-1α protein. *J Biol Chem*. 2010;285:32116-32125.
53. Jazwa A, Stoszko M, Tomczyk M, Bukowska-Strakova K, Pichon C, Jozkowicz A and Dulak J. HIF-regulated HO-1 gene transfer improves the post-ischemic limb recovery and diminishes TLR-triggered immune responses - Effects modified by concomitant VEGF overexpression. *Vascul Pharmacol*. 2015;71:127-138.
54. Chalothorn D and Faber JE. Strain-dependent variation in collateral circulatory function in mouse hindlimb. *Physiol Genomics*. 2010;42:469-479.
55. Dutta P, Courties G, Wei Y, Leuschner F, Gorbatov R, Robbins CS, Iwamoto Y, Thompson B, Carlson AL, Heidt T, Majmudar MD, Lasitschka F, Etzrodt M, Waterman P, Waring MT, Chicoine AT, van der Laan AM, Niessen HW, Piek JJ, Rubin BB, Butany J, Stone JR, Katus HA, Murphy SA, Morrow DA, Sabatine MS, Vinegoni C, Moskowitz MA, Pittet MJ, Libby P, Lin CP, Swirski FK, Weissleder R and Nahrendorf M. Myocardial infarction accelerates atherosclerosis. *Nature*. 2012;487:325-329.
56. Dunn LL, Midwinter RG, Ni J, Hamid HA, Parish CR and Stocker R. New insights into intracellular locations and functions of heme oxygenase-1. *Antioxid Redox Signal*. 2014;20:1723-1742.
57. Kitamuro T, Takahashi K, Ogawa K, Udono-Fujimori R, Takeda K, Furuyama K, Nakayama M, Sun J, Fujita H, Hida W, Hattori T, Shirato K, Igarashi K and Shibahara S. Bach1 functions as a hypoxia-inducible repressor for the heme oxygenase-1 gene in human cells. *J Biol Chem*. 2003;278:9125-9133.
58. Singh C, Hoppe G, Tran V, McCollum L, Bolok Y, Song W, Sharma A, Brunengraber H and Sears JE. Serine and 1-carbon metabolism are required for HIF-mediated protection against retinopathy of prematurity. *JCI Insight*. 2020;4:e129398.
59. Kim JW, Tchernyshyov I, Semenza GL and Dang CV. HIF-1-mediated expression of pyruvate dehydrogenase kinase: a metabolic switch required for cellular adaptation to hypoxia. *Cell Metab*. 2006;3:177-185.
60. Boström P, Magnusson B, Svensson PA, Wiklund O, Borén J, Carlsson LM, Ståhlman M, Olofsson SO and Hultén LM. Hypoxia converts human macrophages into triglyceride-loaded foam cells. *Arterioscler Thromb Vasc Biol*. 2006;26:1871-1876.
61. Yurkov YA and Safonova TY. Effect of hypoxia on nicotinamide coenzyme content in tissues of newborn rats. *Bull Exp Biol Med*. 1976;82:1656–1658.
62. Rey S, Luo W, Shimoda LA and Semenza GL. Metabolic reprogramming by HIF-1 promotes the survival of bone marrow-derived angiogenic cells in ischemic tissue. *Blood*. 2011;117:4988-4998.
63. Ogle ME, Gu X, Espinera AR and Wei L. Inhibition of prolyl hydroxylases by dimethyloxaloylglycine after stroke reduces ischemic brain injury and requires hypoxia inducible factor-1α. *Neurobiol Dis*. 2012;45:733-742.

Highlights

- Heme oxygenase-1 (Hmox1) deficiency promotes auto-amputation following hind limb ischemia
- Heme oxygenase-1 stabilizes hypoxia-inducible factor-1α (HIF-1α)
- Stabilization of HIF-1α rescues ischemia-induced auto-amputation in Hmox1 deficiency
- Carbon monoxide, the product of Hmox1 enzymatic activity, stabilizes HIF-1α

Figure Legends

Figure 1. Hmox1 deficiency is associated with ischemia–induced auto-amputation and impaired blood flow recovery. Unilateral hind limb ischemia was surgically induced in male and female *Hmox1*$^{+/+}$ and *Hmox1*$^{-/-}$ mice, with sham preparation of the contralateral limb. **(A)** Representative photographs of sham-operated (S) and ischemic (I) hind limbs. **(B)** Incidence of auto-amputation. **(C)** Tissue injury score: 0, normal; 1, mild discoloration; 2, necrosis; 3, auto-amputation below the ankle; 4, auto-amputation above the ankle. **(D)** Pedal reflex score: 0, normal; 1, plantar but not toe flexion; 2, no flexion; 3, dragging of foot; 4, dragging of limb. **(E)** Representative laser Doppler perfusion images

with red pixels indicating maximal perfusion. **(F)** Laser Doppler blood perfusion ratio in the ischemic versus non-ischemic hind limb. **(G)** Vessel density per myocyte grouped by lumen diameter (<50 μm, 50-100 μm, >100 μm) in gastrocnemius tissue. Data were enumerated by blinded observers and are expressed as mean ± SEM, n=10 per genotype. Results in **(B)-(D)** and **(F)** were assessed by 2-way ANOVA with repeated measures in **(C)-(D)** by Sidak's multiple comparison test, and in **(G)** by Mann-Whitney test, *P<0.05.

Figure 2. Hmox1 in bone marrow cells does not fully rescue auto-amputations in response to ischemia. Bone marrow transfer experiments were performed between male *Hmox1*$^{+/+}$ donors and irradiated female *Hmox1*$^{+/+}$ or *Hmox1*$^{-/-}$ recipients. At 42 d post-transfer, unilateral hind limb ischemia was surgically induced with sham preparation of the contralateral limb. **(A)** Incidence of auto-amputation. **(B)** Tissue injury score: 0, normal; 1, mild discoloration; 2, necrosis; 3, auto-amputation below the ankle; 4, auto-amputation above the ankle. **(C)** Pedal reflex score: 0, normal; 1, plantar but not toe flexion; 2, no flexion; 3, dragging of foot; and 4, dragging of limb. **(D)** Laser Doppler blood perfusion ratio in the ischemic versus non-ischemic hind limb. **(E)** Vessel density per myocyte grouped by lumen diameter (<50 μm, 50-100 μm, >100 μm) in gastrocnemius tissue. Data were enumerated by blinded observers and are expressed as mean ± SEM, n=6-7 per genotype. Results in **(A)-(D)** were assessed by 2-way ANOVA with repeated measures in **(B)-(D)** by Sidak's multiple comparison test, and in **(E)** by Mann-Whitney test, *P<0.05.

Figure 3. Hmox1 affects energy metabolism and glucose utilization in response to ischemia. Unilateral hind limb ischemia was surgically induced in male and female *Hmox1*$^{+/+}$ and *Hmox1*$^{-/-}$ mice with sham preparation of the contralateral limb as indicated. **(A)** Maximal oxidative phosphorylation (P_{MAX}), and **(B)** electron transfer capacity through complex I (P_{CI}), complex II (P_{CII}), electron transferring flavoprotein (P_{ETF}) and uncoupled oxidative phosphorylation (ETS) in red naïve muscle fibers of gastrocnemius determined by high-resolution respirometry in naïve mice. **(C)** Glucose utilization in soleus of naïve mice as determined by *ex vivo* [^{3}H]-2-deoxyglucose uptake. **(D)** Maximal oxidative phosphorylation (P_{MAX}), and **(E)** electron transfer capacity through complex I (P_{CI}), complex II (P_{CII}), electron transferring flavoprotein (P_{ETF}) and uncoupled oxidative phosphorylation (ETS) in red ischemic muscle fibers of gastrocnemius determined by high-resolution respirometry 3 days post ischemia. **(F)** Glucose utilization in soleus of ischemic mice 3 days after ischemia as determined by *ex vivo* [^{3}H]-2-deoxyglucose uptake. Glucose utilization **(G)**, plasma lactate **(H)** and maximal oxidative phosphorylation (P_{MAX}) in red sham-operated muscle fibers of gastrocnemius (**I**) in ischemic mice with data in **(G)-(H)** expressed as a fold change of naïve mice. **(J)** Hmox1 protein expression in red sham-operated muscle of gastrocnemius. Data are expressed as mean ± SEM, n=3-12 mice per genotype. Results in **(C)** assessed by unpaired *t*-test, **(G)-(H)** assessed by 2-way ANOVA, **(I)** assessed by Mann-Whitney test, *P<0.05 compared to naïve *Hmox1*$^{+/+}$ mice.

Figure 4. Hmox1 stabilizes HIF-1α in response to ischemia. Unilateral hind limb ischemia was surgically induced in male and female *Hmox1*$^{+/+}$ and *Hmox1*$^{-/-}$ mice and the ischemic tissues assessed by Western blot for **(A)** HIF-1α and Hmox1 (**B**) using gastrocnemius. Ctrl refers to DMOG-treated muscle **(A)** and hemin-treated mouse endothelial cells (**B**). **(C)** Concentration of biliverdin in tibialis anterior determined by LC-MS/MS. **(D)** qPCR analysis of *Hmox1* mRNA in plantaris. Data are expressed as mean ± SEM, n=3-6 mice per genotype and were assessed by 2-way ANOVA, *P<0.05 compared to naïve (0 h time point) *Hmox1*$^{+/+}$ mice.

Figure 5. Hmox1 stabilizes HIF-1α and is required for the metabolic response to hypoxia *in vitro*. Dermal fibroblasts cultured from *Hmox1*$^{+/+}$ and *Hmox1*$^{-/-}$ mice were exposed to 1% O_2 as indicated. Western blot analysis of **(A)** Hmox1 and **(B)** HIF-1 α. **(C)** [^{3}H]-2-deoxyglucose uptake. Intracellular pyruvate **(D)** and lactate **(E)**. Western blots in **(A)-(B)** are representative of at least 3 fibroblast lines derived independently per genotype. Data are expressed as mean ± SEM and were analyzed by 2-way ANOVA, *P<0.05, compared to *Hmox1*$^{+/+}$ normoxia (0 h time point; air).

Figure 6. DMOG improves HIF-1α stabilization in response to hypoxia in *Hmox1* deficiency. Dermal fibroblasts were cultured from *Hmox1*$^{-/-}$ mice. **(A)** Fibroblasts were treated with media control

or 500 μM DMOG, exposed to 1% O_2 for the time indicated, followed by Western blot analysis of HIF-1α. Data are expressed as mean ± SEM, n=3 and assessed by 2-way ANOVA, *P<0.05. **(B)** Fibroblasts were treated with media control or 500 μM DMOG, 5.8 μM CORM-A1 or iCORM-A1, exposed to 1% O_2 for 30 min, followed by Western blot analysis of HIF-1α. Data are expressed as mean ± SEM, n=7 and were assessed by 1-tailed Mann-Whitney test, *P<0.05, compared to 1% O_2 control. Unilateral hind limb ischemia was surgically induced in *Hmox1*$^{-/-}$ and wild-type littermate mice of both sexes. DMOG (8 mg/mouse; or saline control (Ctrl)) was administered by i.p. injection before surgery then every other day. **(C)** Western blot analysis of HIF-1α in gastrocnemius. **(D)** Incidence of auto-amputation. **(E)** Tissue injury score: 0, normal; 1, mild discoloration; 2, necrosis; 3, auto-amputation below the ankle; 4, auto-amputation above the ankle. **(F)** Laser Doppler blood perfusion ratio in the ischemic versus non-ischemic hind limb. Metabolic pathways of metabolites detected using targeted analysis and significantly altered in **(G)** *Hmox1*$^{-/-}$ mice treated with saline (n=2) compared to *Hmox1*$^{-/-}$ mice treated with DMOG (n=4), and **(H)** *Hmox1*$^{-/-}$ mice treated with saline compared to wild-type mice (n=6). 1CM, 1-carbon metabolism; TCA, tricarboxylic acid cycle; TAG, triglycerides. Data were enumerated by blinded observers and are expressed as mean ± SEM, n=12 per genotype. Results were assessed by Mann-Whitney test in **(C)**, and **(D)-(F)** by 2-way ANOVA with repeated measures in **(E)-(F)** by Sidak's multiple comparison test, *P<0.05.

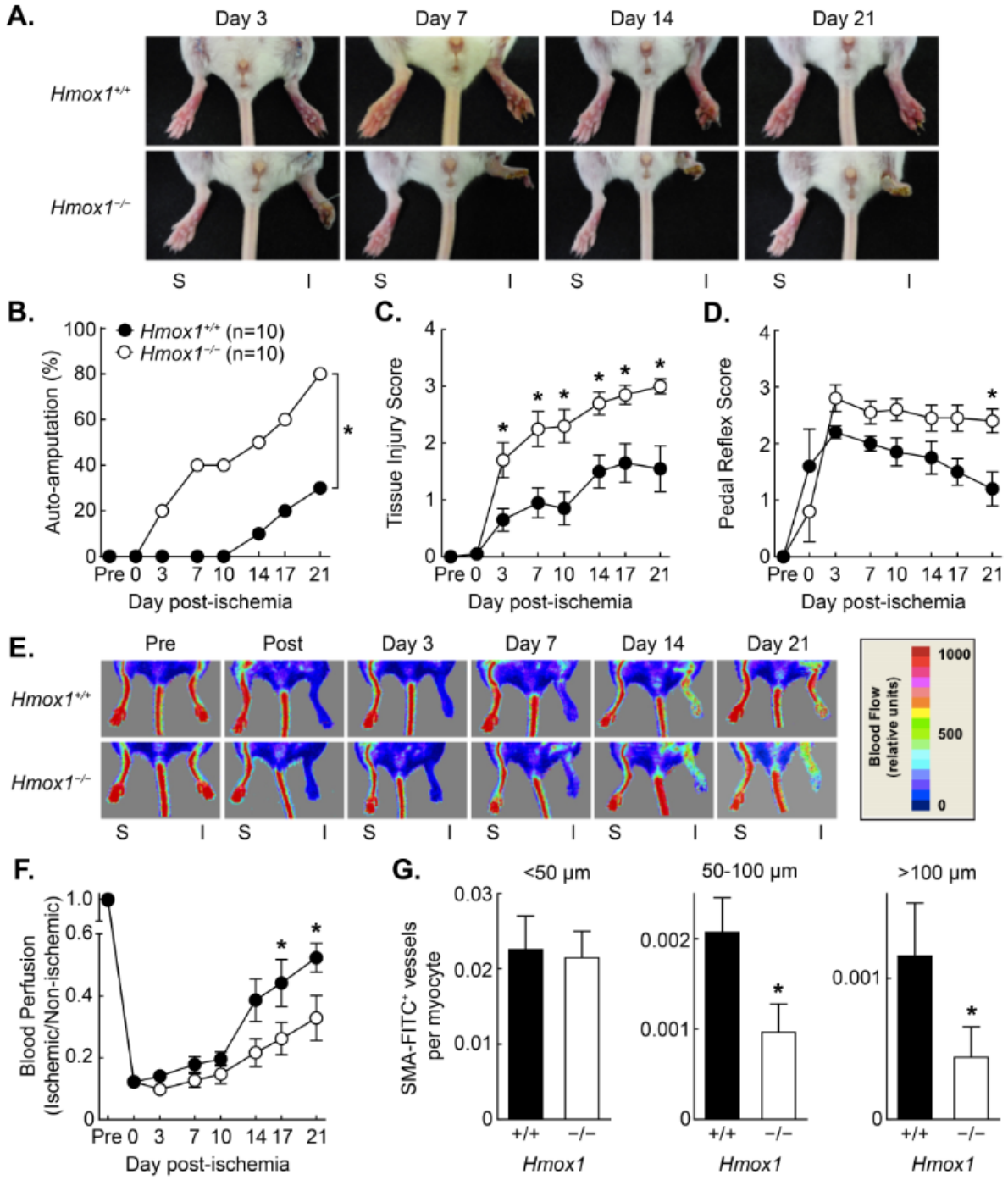
A.
Day 3
Day 7
Day 14
Day 21
Hmox1+/+
Hmox1−/−
S
I
B.
Hmox1+/+ (n=10)
Hmox1−/− (n=10)
Auto-amputation (%)
Pre 0 3 7 10 14 17 21
Day post-ischemia
C.
Tissue Injury Score
Day post-ischemia
D.
Pedal Reflex Score
Day post-ischemia
E.
Pre
Post
Day 3
Day 7
Day 14
Day 21
Blood Flow (relative units)
1000
500
0
F.
Blood Perfusion (Ischemic/Non-ischemic)
Day post-ischemia
G.
<50 µm
50-100 µm
>100 µm
SMA-FITC+ vessels per myocyte
+/+
−/−
Hmox1

Figure 1

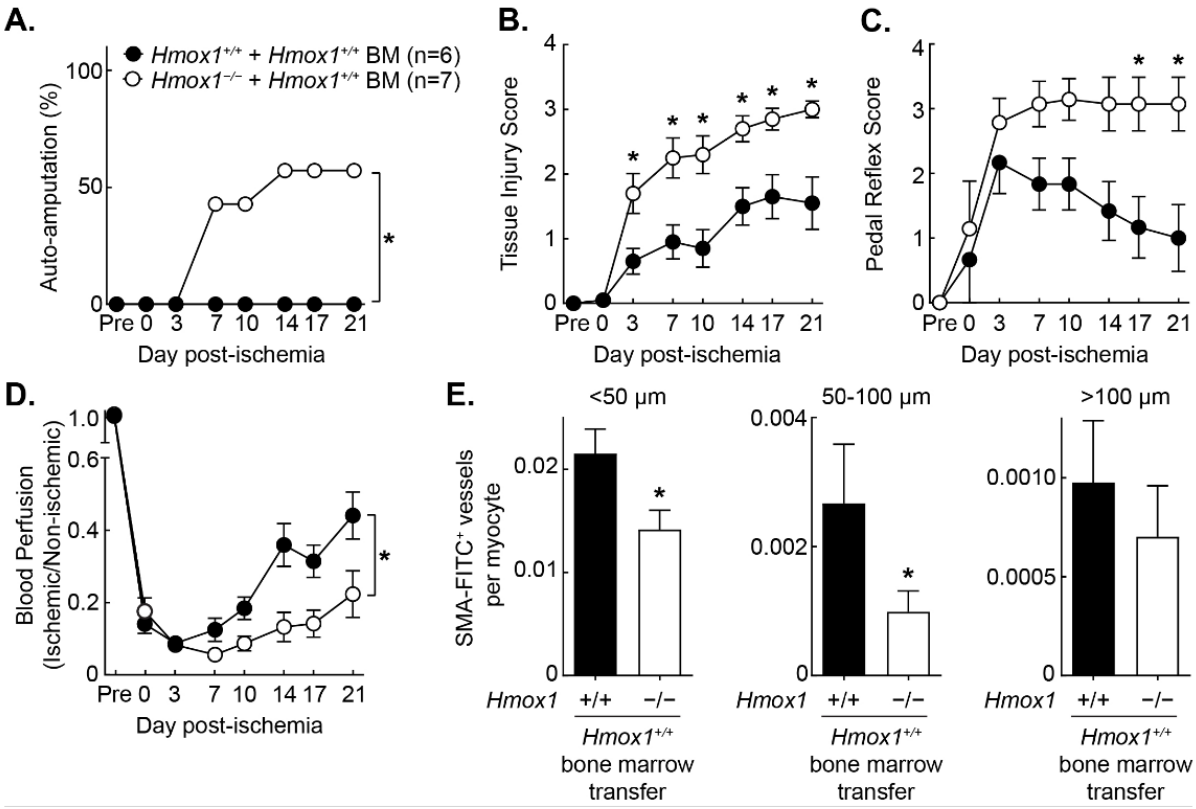
A.
Hmox1+/+ + Hmox1+/+ BM (n=6)
Hmox1−/− + Hmox1+/+ BM (n=7)
Auto-amputation (%)
Day post-ischemia
B.
Tissue Injury Score
Day post-ischemia
C.
Pedal Reflex Score
Day post-ischemia
D.
Blood Perfusion (Ischemic/Non-ischemic)
Day post-ischemia
E.
<50 µm
50-100 µm
>100 µm
SMA-FITC+ vessels per myocyte
Hmox1 +/+ −/−
Hmox1+/+ bone marrow transfer

Figure 2

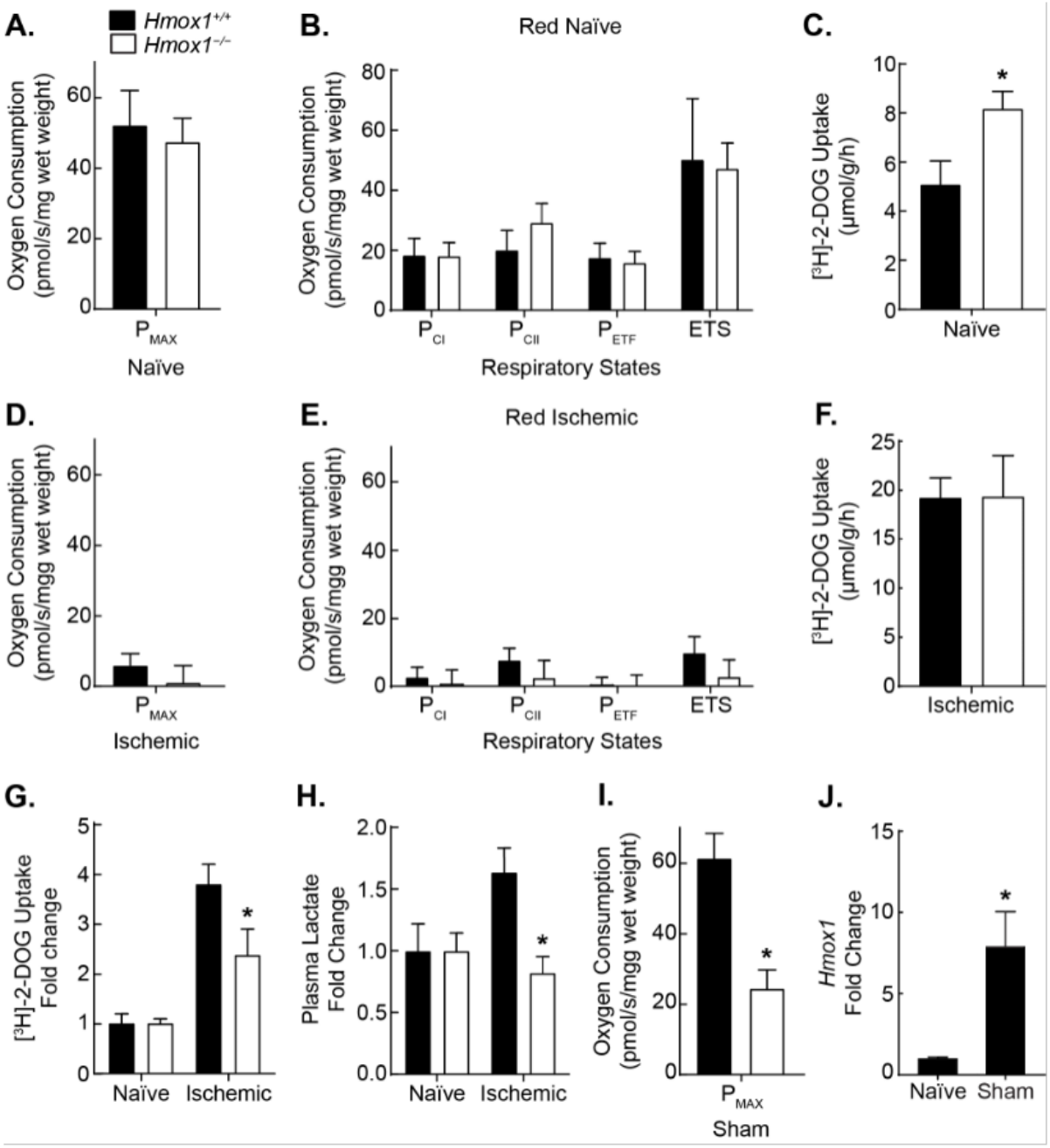
A.
Hmox1+/+
Hmox1−/−
Oxygen Consumption (pmol/s/mg wet weight)
P MAX
Naïve
B.
Red Naïve
Oxygen Consumption (pmol/s/mgg wet weight)
P CI
P CII
P ETF
ETS
Respiratory States
C.
[3H]-2-DOG Uptake (µmol/g/h)
Naïve
D.
Oxygen Consumption (pmol/s/mgg wet weight)
P MAX
Ischemic
E.
Red Ischemic
Oxygen Consumption (pmol/s/mgg wet weight)
P CI
P CII
P ETF
ETS
Respiratory States
F.
[3H]-2-DOG Uptake (µmol/g/h)
Ischemic
G.
[3H]-2-DOG Uptake Fold change
Naïve
Ischemic
H.
Plasma Lactate Fold Change
Naïve
Ischemic
I.
Oxygen Consumption (pmol/s/mgg wet weight)
P MAX
Sham
J.
Hmox1 Fold Change
Naïve
Sham

Figure 3

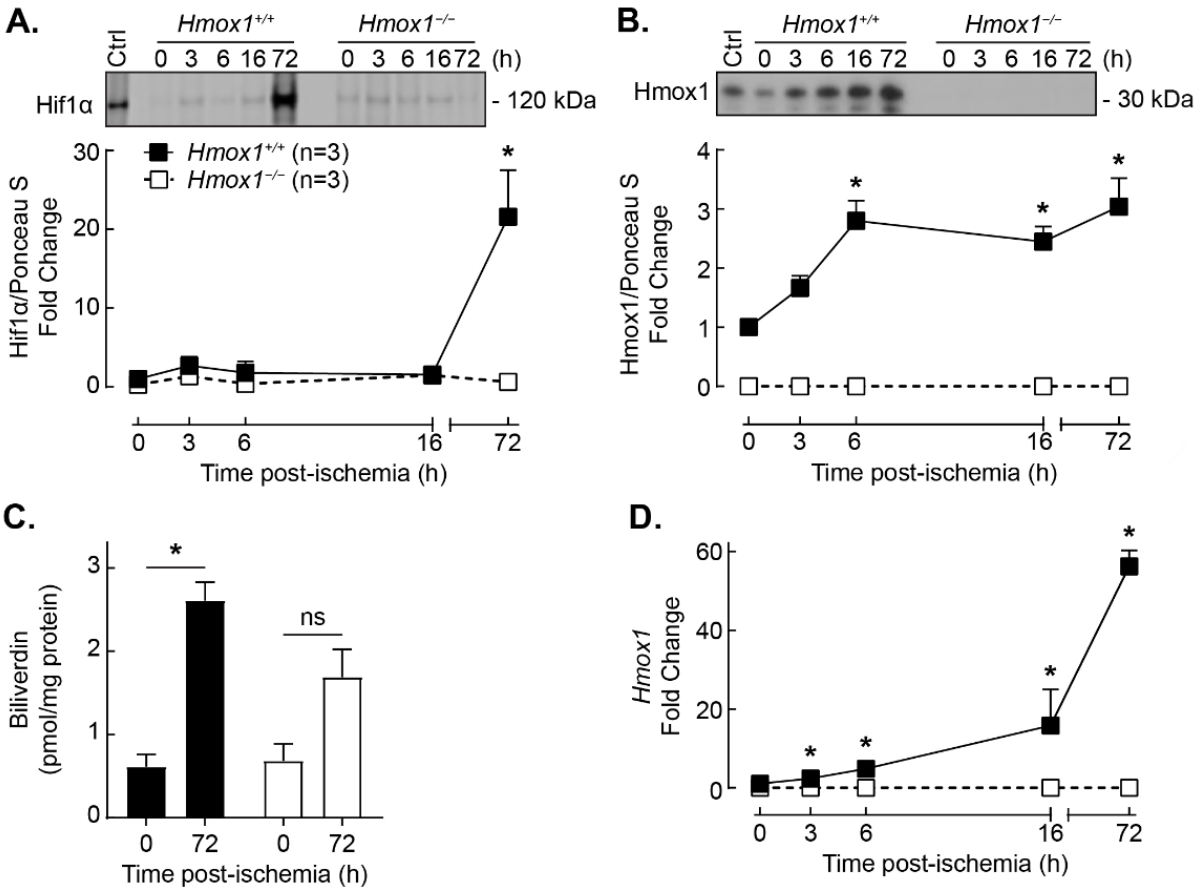
A.
Ctrl
Hmox1+/+
Hmox1−/−
0 3 6 16 72 (h)
Hif1α
- 120 kDa
Hmox1+/+ (n=3)
Hmox1−/− (n=3)
Hif1α/Ponceau S Fold Change
Time post-ischemia (h)
B.
Hmox1
- 30 kDa
Hmox1/Ponceau S Fold Change
C.
Biliverdin (pmol/mg protein)
ns
D.
Hmox1 Fold Change

Figure 4

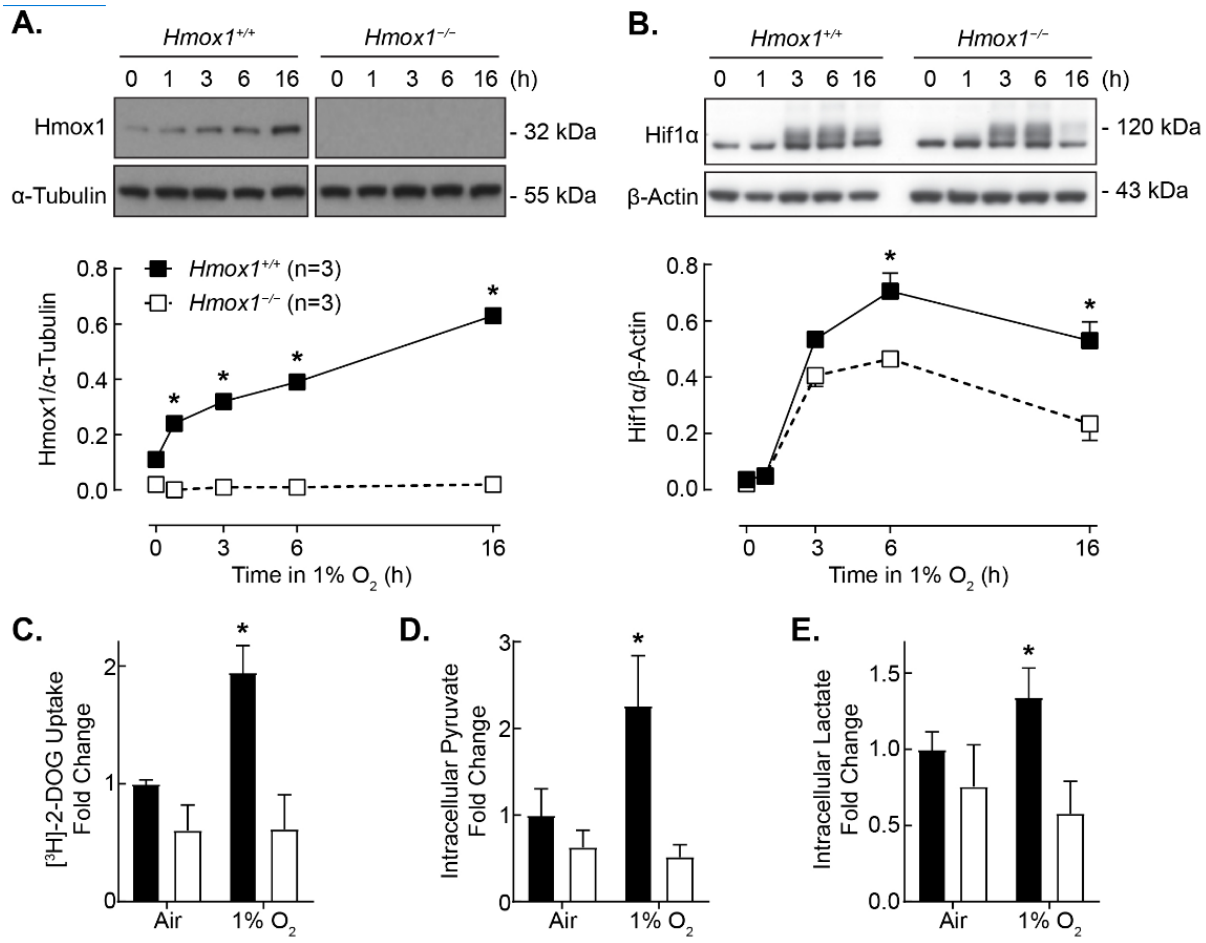
A.
Hmox1+/+
Hmox1−/−
0 1 3 6 16 0 1 3 6 16 (h)
Hmox1
- 32 kDa
α-Tubulin
- 55 kDa
B.
Hmox1+/+
Hmox1−/−
0 1 3 6 16 0 1 3 6 16 (h)
Hif1α
- 120 kDa
β-Actin
- 43 kDa
Hmox1/α-Tubulin
Hmox1+/+ (n=3)
Hmox1−/− (n=3)
Time in 1% O2 (h)
Hif1α/β-Actin
Time in 1% O2 (h)
C.
[3H]-2-DOG Uptake Fold Change
Air
1% O2
D.
Intracellular Pyruvate Fold Change
Air
1% O2
E.
Intracellular Lactate Fold Change
Air
1% O2

Figure 5

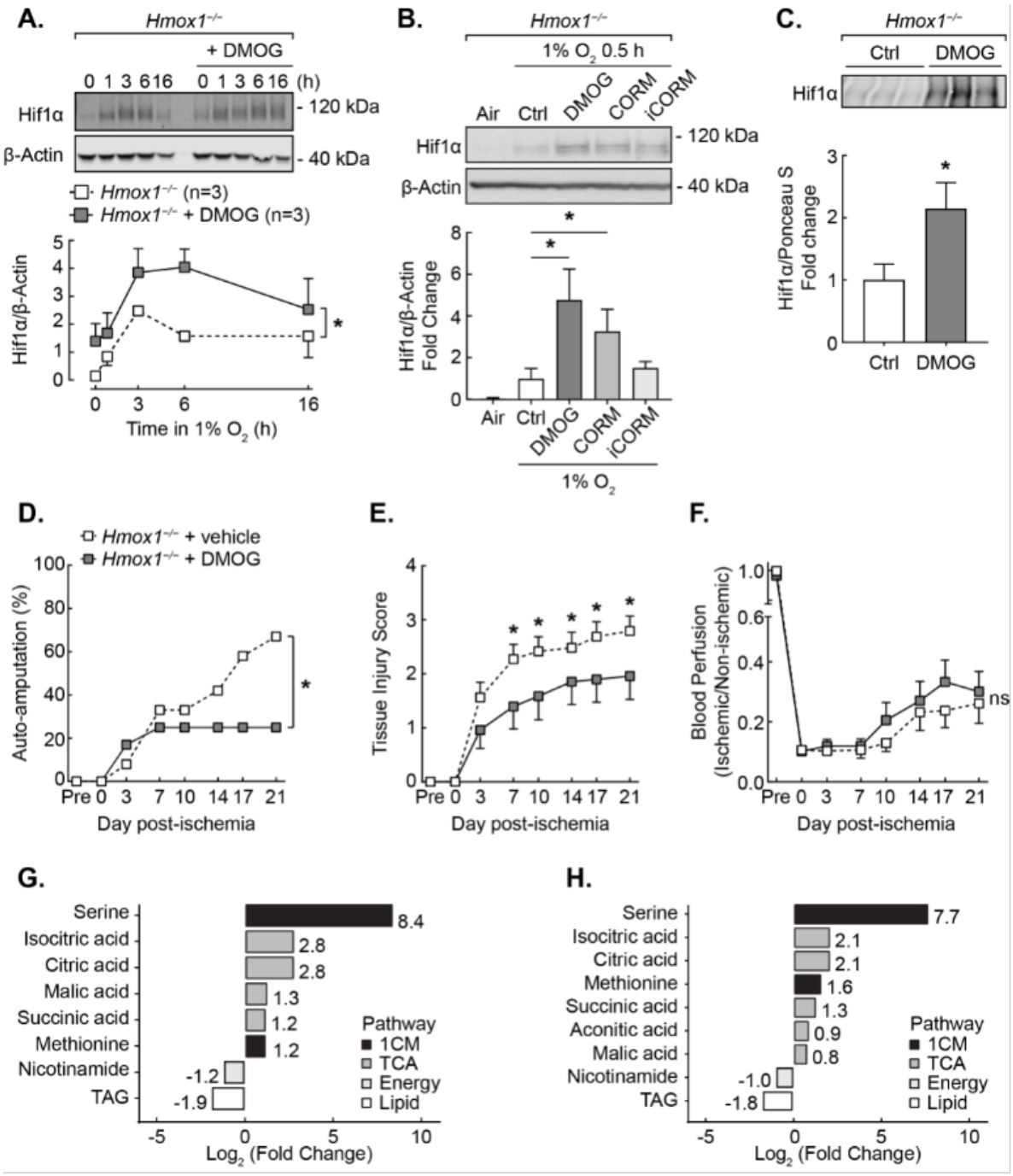
A.
Hmox1−/−
+ DMOG
0 1 3 6 16 0 1 3 6 16 (h)
Hif1α
- 120 kDa
β-Actin
- 40 kDa
Hmox1−/− (n=3)
Hmox1−/− + DMOG (n=3)
Hif1α/β-Actin
Time in 1% O2 (h)
B.
Hmox1−/−
1% O2 0.5 h
Air Ctrl DMOG CORM iCORM
Hif1α
- 120 kDa
β-Actin
- 40 kDa
Hif1α/β-Actin Fold Change
1% O2
C.
Hmox1−/−
Ctrl DMOG
Hif1α
Hif1α/Ponceau S Fold change
D.
Hmox1−/− + vehicle
Hmox1−/− + DMOG
Auto-amputation (%)
Day post-ischemia
E.
Tissue Injury Score
Day post-ischemia
F.
Blood Perfusion (Ischemic/Non-ischemic)
ns
Day post-ischemia
G.
Serine 8.4
Isocitric acid 2.8
Citric acid 2.8
Malic acid 1.3
Succinic acid 1.2
Methionine 1.2
Nicotinamide -1.2
TAG -1.9
Pathway
1CM
TCA
Energy
Lipid
Log2 (Fold Change)
H.
Serine 7.7
Isocitric acid 2.1
Citric acid 2.1
Methionine 1.6
Succinic acid 1.3
Aconitic acid 0.9
Malic acid 0.8
Nicotinamide -1.0
TAG -1.8
Pathway
1CM
TCA
Energy
Lipid
Log2 (Fold Change)

Figure 6